

Behavioral/Cognitive

Rapid Processing of Invisible Fearful Faces in the Human Amygdala

Yingying Wang,^{1*} Lu Luo,^{2*} Guanpeng Chen,^{3,4,5} Guoming Luan,^{6,7,8} Xiongfei Wang,⁶ Qian Wang,^{3,4,5} and Fang Fang^{3,4,5}

¹Department of Psychology and Behavioral Sciences, Zhejiang University, Hangzhou 310028, Zhejiang, China, ²School of Psychology, Beijing Sport University, Beijing 100084, China, ³School of Psychological and Cognitive Sciences and Beijing Key Laboratory of Behavior and Mental Health, Peking University, Beijing 100871, China, ⁴IDG/McGovern Institute for Brain Research, Peking University, Beijing 100871, China, ⁵Peking-Tsinghua Center for Life Sciences, Peking University, Beijing 100871, China, ⁶Department of Functional Neurosurgery, Sanbo Brain Hospital, Capital Medical University, Beijing 1000932, China, ⁷Beijing Key Laboratory of Epilepsy, Epilepsy Center, Sanbo Brain Hospital, Capital Medical University, Beijing 100093, China, ⁸Beijing Institute for Brain Disorders, Beijing 100069, China, and ⁹Department of Clinical Neuropsychology, Sanbo Brain Hospital, Capital Medical University, Beijing 100093 China

Rapid detection of a threat or its symbol (e.g., fearful face), whether visible or invisible, is critical for human survival. This function is suggested to be enabled by a subcortical pathway to the amygdala independent of the cortex. However, conclusive electrophysiological evidence in humans is scarce. Here, we explored whether the amygdala can rapidly encode invisible fearful faces. We recorded intracranial electroencephalogram (iEEG) responses in the human (both sexes) amygdala to faces with fearful, happy, and neutral emotions rendered invisible by backward masking. We found that a short-latency intracranial event-related potential (iERP) in the amygdala, beginning 88 ms poststimulus onset, was preferentially evoked by invisible fearful faces relative to invisible happy or neutral faces. The rapid iERP exhibited selectivity to the low spatial frequency (LSF) component of the fearful faces. Time-frequency iEEG analyses further identified a rapid amygdala response preferentially for LSF fearful faces at the low gamma frequency band, beginning 45 ms poststimulus onset. In contrast, these rapid responses to invisible fearful faces were absent in cortical regions, including early visual areas, the fusiform gyrus, and the parahippocampal gyrus. These findings provide direct evidence for the existence of a subcortical pathway specific for rapid fear detection in the amygdala and demonstrate that the subcortical pathway can function without conscious awareness and under minimal influence from cortical areas.

Key words: amygdala intracranial electroencephalogram; low spatial frequency; subcortical pathway; unconscious

Significance Statement

Automatic detection of biologically relevant stimuli, such as threats or dangers, has remarkable survival value. Here, we provide direct intracranial electrophysiological evidence that the human amygdala preferentially responds to fearful faces at a rapid speed, despite the faces being invisible. This rapid, fear-selective response is restricted to faces containing low spatial frequency information transmitted by magnocellular neurons and does not appear in cortical regions. These results support the existence of a rapid subcortical pathway independent of cortical pathways to the human amygdala.

Received July 1, 2022; revised Dec. 4, 2022; accepted Dec. 29, 2022.

Author contributions: Y.W., L.L., and F.F. designed research; Y.W., L.L., G.C., G.L., X.W., and Q.W. performed research; Y.W., L.L., and Q.W. analyzed data; and Y.W., Q.W., and F.F. wrote the paper.

This work was supported by STI2030-Major Projects 2022ZD0204800, National Natural Science Foundation of China Grant 31930053, and Beijing Academy of Artificial Intelligence (F.F.); STI2030-Major Projects 2022ZD0204800 and National Natural Science Foundation of China Grant 32171039 (Q.W.); and National Natural Science Foundation of China Grant 32100838 (Y.W.). We thank Pengfei Teng and Jing Wang for assistance in data acquisition and analysis.

*Y.W. and L.L. contributed equally to this work.

The authors declare no competing financial interests.

Correspondence should be addressed to Fang Fang at ffang@pku.edu.cn or Qian Wang at wangqiansy@pku.edu.cn.

<https://doi.org/10.1523/JNEUROSCI.1294-22.2022>

Copyright © 2023 the authors

Introduction

The ability to rapidly process emotional signals, whether visible or invisible, may offer an evolutionary advantage in enabling threat detection. The amygdala is suggested to play a key role in this process. Human brain imaging studies have shown elevated amygdala activities to threat-related stimuli, such as fearful faces (Phan et al., 2002), even when the stimuli are invisible (Whalen et al., 1998; Morris et al., 1998b; Williams et al., 2004) or presented to cortically blind patients (Morris et al., 2001; Tamietto et al., 2009). However, being unable to measure very fast neural responses in deep brain structures, traditional brain imaging techniques only provide indirect evidence for rapid fear processing in the amygdala. Taking advantage of

Table 1. Patient demographic and iEEG recording contacts

Patient No.	Sex	Hand edness	Age	Age of epilepsy	Amygdala contacts*	EVA contacts*	FG contacts*	PHG contacts*	Etiology	Lesion location
02	M	R	19	8	4 (R)	4 (R), 3 (R)		2 (R), 3 (R)	ganglioglioma	Right middle/inferior temporal lobe, right hippocampus, right parahippocampus
05	M	R	34	20	3 (R)				MRI negative	Right middle/inferior temporal lobe, right hippocampus, right amygdala
06	F	R	46	40			2 (L)		MRI negative	Left superior temporal gyrus
07	F	R	44	32	2 (R)				MRI negative	Bilateral temporal lobe
08	F	R	31	18	3 (L)				MRI negative	Right inferior temporal lobe, right hippocampus, right amygdala
10	M	R	35	4		2 (L)			Encephalomalacia	Left posterior temporal lobe
12	M	R	27	13	4 (R)		2 (R)		Focal dysplasia	Right middle/inferior temporal lobe, right hippocampus
13	F	R	32	31		8 (L)		4 (L)	MRI negative	Left anterior cingulate gyrus
14	M	R	23	12	4 (R)	2 (L), 2 (L)	3 (L)	3 (L), 1 (L)	Left hippocampal sclerosis	Left inferior temporal lobe, left hippocampus, left amygdala
15	M	R	19	13	4 (L)	4 (L)			Encephalitis; focal dysplasia	Right temporal lobe, right occipital lobe
16	M	R	38	30		3 (R)	3 (L), 3 (R)	1 (L)	Encephalitis	Left hippocampus
17	M	R	35	31	4 (L), 2 (R)				MRI negative	Bilateral temporal lobe
18	F	R	45	22	3 (R)				MRI negative	Right superior temporal gyrus

*Number of contacts in an electrode. M, Male; F, female; L, left; R, right.

intracranial electroencephalogram (iEEG), which enables the direct electrophysiological recording with a high temporal resolution in the amygdala, a previous study has revealed fear-selective amygdala responses occurring at a rapid speed (Méndez-Bértolo et al., 2016). However, whether such a rapid amygdala response occurs with invisible fear is still unknown.

Based on rodent research (LeDoux, 1996), a low-road model suggests that rapid fear detection in the amygdala is enabled through a subcortical pathway, which transmits coarse information through the superior colliculus and pulvinar to the amygdala, bypassing the typically time-consuming cortical pathways (Tamietto and de Gelder, 2010). Alternatively, a multiroad model proposes that cortical pathways, which contain a multitude of shortcut anatomic routes relaying visual information to the amygdala from the extrastriate visual cortex, can be equally fast at transmitting fear as the subcortical pathway (Pessoa and Adolphs, 2010). As such, the evidence of rapid amygdala response alone cannot discriminate between the two models. To identify the contribution of the subcortical pathway, rapid amygdala response should be examined after minimizing the information transmission in cortical areas.

Unconscious fear processing offers a way to minimize information transmission and processing through cortices while retaining the subcortical contribution. The subcortical pathway is more sensitive than the cortical pathway to invisible stimuli (Tamietto and de Gelder, 2010; Diano et al., 2017). Invisible stimuli are either insufficient to evoke cortical responses or evoke much weaker responses than visible stimuli (Tamietto and de Gelder, 2010). On the contrary, invisible stimuli can evoke equal or even stronger responses in subcortical structures, including the amygdala, superior colliculus, and pulvinar, relative to visible stimuli (Morris et al., 1999; Brooks et al., 2012; Axelrod et al., 2015). Unconscious emotion processing may even adaptively increase the involvement of the subcortical pathway, as destruction of visual cortices strengthens anatomic connections of brain structures along the subcortical pathway (Tamietto et al., 2012). Furthermore, the subcortical and cortical pathways dissociate on their responses to low and high spatial frequency information. Specifically, although the cortical pathway is preferentially sensitive to the high spatial frequency information, the subcortical pathway responds to the low spatial frequency information as it carries visual inputs to the

amygdala via magnocellular neurons (Vuilleumier et al., 2003). Therefore, if a low road exists, rapid threat detection should be observed in the amygdala for low spatial frequency information independent of stimulus visibility and cortical involvement. If multiple cortical routes are recruited as proposed by the multiroad model, rapid threat detection in the amygdala would not be observed for invisible stimuli.

To explore the characteristics and temporal dynamics of the amygdala response to invisible fear while minimizing cortical contributions, here, we recorded iEEG signals in patients with medication-resistant epilepsy while they were presented with fearful, happy, or neutral faces rendered invisible by backward masking. The faces were presented in their intact format—broad spatial frequency (BSF)—or were spatially filtered to contain only their low spatial frequency (LSF) or high spatial frequency (HSF) components. Electrode contacts were localized in the amygdala and cortical areas along the ventral visual pathway. We identified an early iERP and an early low gamma band response in the amygdala specific to invisible LSF fearful faces, supporting the existence of a fast subcortical pathway that deals with unconscious threats.

Materials and Methods

Subjects

Subjects were 18 patients (13 males, all right handed, 19–46 years old) with pharmacologically intractable epilepsy (Table 1). Among them, 13 were implanted with amygdala electrodes, 7 with fusiform gyrus (FG) electrodes, 8 with parahippocampal gyrus (PHG) electrodes, and 9 with early visual area (EVA; i.e., V1, V2, and V3) electrodes. They were admitted to the Sanbo Brain Hospital, Capital Medical University, to localize seizure foci for potential surgical resection. The study was performed 3 or 3 d after the stereotactic electrode implantation. All patients had self-reported normal vision and provided written informed consent for their participation. The experimental procedure was approved by the Ethics Committee of the Sanbo Brain Hospital of Capital Medical University and the Human Subject Review Committee of Peking University. No statistical method was used to predetermine the sample size, but our sample size is similar to those reported in previous studies (Oya et al., 2002; Krolak-Salmon et al., 2004; Sato et al., 2011; Méndez-Bértolo et al., 2016).

Recording

Each electrode had 10–18 independent recording contacts (0.8 mm in diameter, 2 mm in length, spacing 3.5 mm apart; Huake Hengsheng Medical Technology; Lu et al., 2021). The signal from each recording

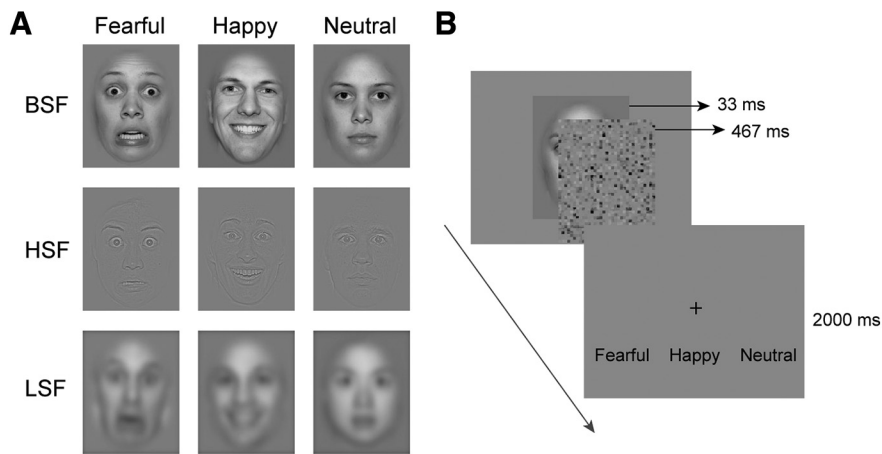


Figure 1. Stimuli and procedure. **A**, Examples of BSF, HSF, and LSF face images with fearful, happy, or neutral emotion. **B**, A face image was presented for 33 ms, followed by a 467 ms white noise mask to prevent awareness of the face. Patients were instructed to identify the facial emotion and make a response within 2000 ms.

Table 2. Emotion discrimination performance in each condition

	Accuracy (%)			d'		
	Fearful	Happy	Neutral	Fearful	Happy	Neutral
LSF	21.53 (13.13)	26.62 (12.00)	38.19 (22.05)	0.18 (0.33)	0.13 (0.23)	0.05 (0.12)
HSF	22.45 (11.87)	21.30 (11.87)	39.58 (25.19)	0.25 (0.31)	0.09 (0.24)	−0.00 (0.29)
BSF	38.89 (17.74)	52.08 (23.78)	44.21 (26.84)	0.70 (0.88)	1.19 (1.21)	0.86 (1.04)

Numbers in parentheses are SDs across patients.

contact was amplified using a Nicolet clinical amplifier. iEEG data at each electrode contact site were sampled at 256 Hz for one patient and 512 Hz for the remaining patients. All signals were online high-pass filtered at 0.16 Hz using a two-way least-squares finite impulse response filter and referenced to a forehead scalp electrode. Implantation sites of the EEG electrodes were determined exclusively by clinical criteria.

Stimuli

We compiled the faces of 96 different actors (48 females) posing with fearful, happy, and neutral expressions from two databases, Radboud Faces Database (<https://rafd.socsci.ru.nl/RaFD2/RaFD?p=main>) and NimStim Set of Facial Expressions (<https://danlab.psychology.columbia.edu/content/nimstim-set-facial-expressions>). Images were processed following the procedure by McFadyen et al. (2017). Specifically, all images were gray scaled, equalized in mean luminance, reshaped into the same size ($5^\circ \times 6.3^\circ$), and cropped to exclude most hair and background. To create faces containing low or high spatial frequency information, the original face images (BSF) were filtered using a low-pass cutoff of <6 cycles per image (LSF) and a high-pass cutoff of >24 cycles per image (HSF), respectively. Each identity appeared in all nine conditions (3 emotions \times 3 spatial frequencies). For each patient, 432 images were randomly selected from the image set, resulting in 48 images per condition. Faces with the same emotion and spatial frequency should not appear more than three times in a row. Visual stimuli were presented using MATLAB (MathWorks) software with Psychtoolbox-3 extensions (Brainard, 1997).

Experimental design

Faces were centrally displayed on an LCD screen (refresh rate, 60 Hz) for 33 ms, followed by a 467 ms white noise mask, whose mean luminance matched that of the face images (Fig. 1). A fixation cross was then presented on the screen for 2000 ms, during which patients judged whether the facial expression was fearful, happy, or neutral via key pressing. This forced-choice emotion-discrimination task was used as an objective criterion to assess emotion awareness. A chin set was used to keep the viewing distance and to keep the patient's head as still as possible. Patients were asked to avoid verbalization and minimize eye blinks. The

experiment consisted of three blocks, each consisting of 144 trials and lasting ~ 6 min. Patients took a break after each block.

Data analysis

Patient inclusion. Of the 13 patients with amygdala electrodes, three were excluded because of excessive noise in their iEEG signal or failure to identify any discernible stimulus-evoked components during the 500 ms post-onset interval. To ensure the invisibility of masked faces, we compared each patient's performance in the forced-choice test to the one-tailed 5% cutoff (39%) of the chance distribution of correct choices (Degonda et al., 2005). One patient's performance exceeded this cutoff in emotion discrimination of LSF and HSF faces and was excluded. Despite the short presentation duration and the backward masking effect, we found that $\sim 50\%$ of the patients exceeded the chance distribution cutoff in emotion judgment for BSF facial expressions. So, BSF faces were not used in the

iEEG experiment. Furthermore, contacts that were in the seizure onset zone or severely contaminated by epileptic activity were removed. Overall, nine patients with amygdala electrodes (10 electrodes with 33 contacts) were retained. Using the same inclusion criteria as above, six patients with EVA electrodes (8 electrodes with 28 contacts; V1, 16 contacts; V2, 8 contacts; V3, 4 contacts), four patients with FG electrodes (5 electrodes with 13 contacts), and four patients with PHG electrodes (6 electrodes with 14 contacts) were retained (Table 1).

Electrode localization. To localize the electrodes, we integrated the anatomic information of the brain provided by preoperative magnetic resonance imaging (MRI) and the position information of the electrodes provided by postoperative computer tomography (CT). For each patient, we first coregistered the postimplant CT with the preimplant anatomic T1-weighted MRI for each patient using SPM12 software (<https://www.fil.ion.ucl.ac.uk/spm/software/spm12/>). We then identified electrode traces in the aligned CT images and calculated the coordinates of contacts in Brainstorm (<http://neuroimage.usc.edu/brainstorm>; Tadel et al., 2011). To assign the anatomic label to each contact, we performed subcortical and cortical segmentations based on individual preoperative T1 MRI using FreeSurfer version 6.0 (Dale et al., 1999). We identified amygdala contacts as those localized in the amygdala and further verified them in each patient's native T1 space. An anatomic atlas for retinotopic visual areas V1–V3 (Benson et al., 2014) was used to locate EVA contacts. A high-resolution single-subject atlas (USCBrain; Joshi et al., 2022) was used to locate FG and PHG contacts. To identify cortical contacts, we projected each contact to the nearest vertex on the individual cortical surface using MATLAB function *dnsearch* and assigned the contact to a cortical area based on the projected vertex. For illustration purposes, the coordinates of contacts were normalized to the MNI space and visualized on the template brain *cvs_avg35_inMNI152*.

Preprocessing. Preprocessing was performed using the FieldTrip toolbox (Oostenveld et al., 2011) in MATLAB R2020b. Raw iEEG data from each contact were imported into MATLAB. For each contact of each electrode, epochs from -100 – 500 ms peristimulus onset were extracted from continuous iEEG data. Data epochs containing interictal epileptic spikes or recording artifacts were identified by visual inspection and removed from the analysis. Detrending and baseline correction (100 ms prestimulus baseline) were then performed. No filtering was applied to avoid latency artifacts because of waveform distortion. Finally, epochs were averaged across trials for each experimental condition to obtain iERPs for each contact.

iERP analysis. To determine the time points of significant iERP difference between the fearful/happy faces and the neutral faces in the LSF and HSF conditions, a cluster-based nonparametric permutation test was applied to the iERP amplitude across all contacts (Maris and Oostenveld, 2007). By clustering neighboring samples (i.e., time points) that show the

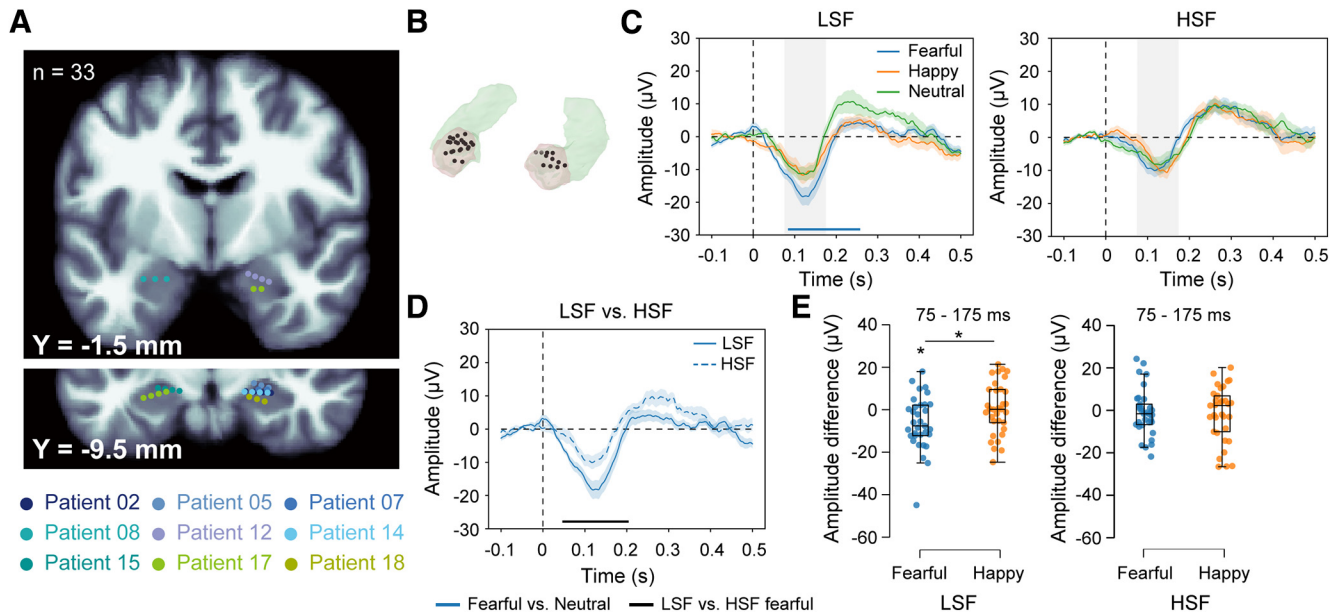


Figure 2. iERPs in the amygdala. **A**, Electrode contact locations in the amygdala for all included patients in coronal sections of the MNI canonical T1 image. Anterior-posterior positions are indicated by Y coordinates. Contacts belonging to the same patient are depicted in the same color. **B**, Electrode contacts (black) in semitransparent segmented amygdalae (beige). **C**, iERPs from 11 amygdalae of nine patients to invisible fearful, happy, and neutral faces with only LSF (left) or HSF (right) components. Bottom, The blue horizontal bar indicates a time cluster that shows significant response differences between the fearful and neutral faces. **D**, iERP comparison between the LSF and HSF fearful faces. Bottom, The black horizontal bar indicates time clusters that show significant response differences between the LSF and HSF fearful faces. The shaded areas around the iERP curves represent the SEM across contacts. **E**, Peak amplitude differences between the LSF/HSF fearful/happy and LSF/HSF neutral faces within the time window of 75–175 ms (gray shaded areas in **C**). The vertical shading in **C** represents the 100-ms time window surrounding the iERP peak. The boxes in box plots show the interquartile range and the median. Whiskers in box plots represent the minimum and maximum in the dataset. * $p < 0.05$ (two-tailed paired t tests, Bonferroni corrected).

same effect, this test deals with the multiple-comparison problem while taking into account the interdependency of the data. For each sample, a paired sample t value was computed. All samples whose t value exceeded the a priori threshold of uncorrected $p < 0.025$ (to correct for the neutral condition being compared twice with fearful/happy conditions) were retained. These t values were subsequently clustered on the basis of temporal adjacency, and the sum of the t values within a cluster was used as the cluster-level statistic. The cluster with the maximum sum was subsequently used as a test statistic. After a permutation step, which randomized the data across the two conditions and recalculated the test statistic 1000 times, we obtained a reference distribution of the maximum cluster-level summed t values to evaluate the statistic of the actual data. Clusters with a t value greater than the 99th percentile ($p < 0.01$) in the permutation distribution were considered significant. The first time point of a significant cluster was then defined as the response latency of the cluster.

To examine the iERP peak amplitude difference across the emotion conditions, we implemented linear mixed-effects models with the lme4 package in R 3.6.3 software. Models were fitted using restricted maximum likelihood. To determine the effect of the predictors of interest, including emotion, spatial frequency, and their interaction, we used the likelihood ratio test to compare models with and without each predictor of interest. The electrodes, amygdala sides, and patients were included as random factors.

Time-frequency analysis. Time-frequency analyses were performed on the epoched iEEG data using continuous Morlet wavelet transformation (function *cwt*) in MATLAB. For each contact, time-frequency maps with a frequency range from 2 to 50 Hz were calculated for each trial; then the amplitudes of the time-frequency maps were averaged across trials. Paired sample t tests comparing the time-frequency maps for the fearful/happy versus neutral faces were performed point-by-point for the amygdala (see Fig. 3A,C), EVA (see Fig. 5A), FG (see Fig. 5B), and PHG (see Fig. 5C) contacts. To reduce false positives, samples with t values exceeding a threshold of $p < 0.005$ were retained. A cluster-based permutation test was then applied with a cluster threshold of $p < 0.05$ (two tailed). For each comparison that showed at least one significant cluster, the earliest time-frequency point of the earliest cluster was defined as the response latency of the comparison effect.

Data availability

Data and codes are available on request from corresponding author Fang Fang at ffang@pku.edu.cn.

Results

Rendering face images invisible

To validate that our backward masking procedure rendered the face images invisible, patients performed an emotion discrimination task. Those who showed an accuracy rate higher than the one-tailed 5% cutoff (39%) of the chance distribution of correct choices (chance level = 33.33%) were excluded (Degonda et al., 2005; see above, Materials and Methods). As shown in Table 2, although the backward masking procedure was effective in blocking the awareness of the LSF (accuracy: mean = 28.78%, SD = 12.32%; d' , mean = 0.12, SD = 0.16) and HSF (accuracy, mean = 27.78%, SD = 11.64%; d' , mean = 0.12; SD = 0.19) faces, it failed to work for the BSF faces (accuracy, mean = 45.06%, SD = 21.08%; d' , mean = 0.92, SD = 1.02), which is in line with previous findings (Pessoa et al., 2005). Therefore, we only included the LSF and HSF faces in the iEEG experiment.

Rapid amygdala responses to invisible fearful faces

We tested 13 patients with amygdala electrodes, nine of whom (10 electrodes with 33 contacts; 6 right, 2 left, and 1 bilateral amygdalae) met our inclusion criteria (Fig. 2A,B, Table 1). To explore amygdala responses to invisible emotions, we compared the fearful/happy versus neutral face processing for the LSF and HSF conditions separately. Cluster-based permutation tests were performed at all time points between -100 and 500 ms around face onset. For the fearful versus neutral face comparison, a significant time cluster was identified at 88 – 256 ms after face onset in the LSF condition; fearful faces induced a more significant iERP response than neutral faces at a cluster threshold of $p <$

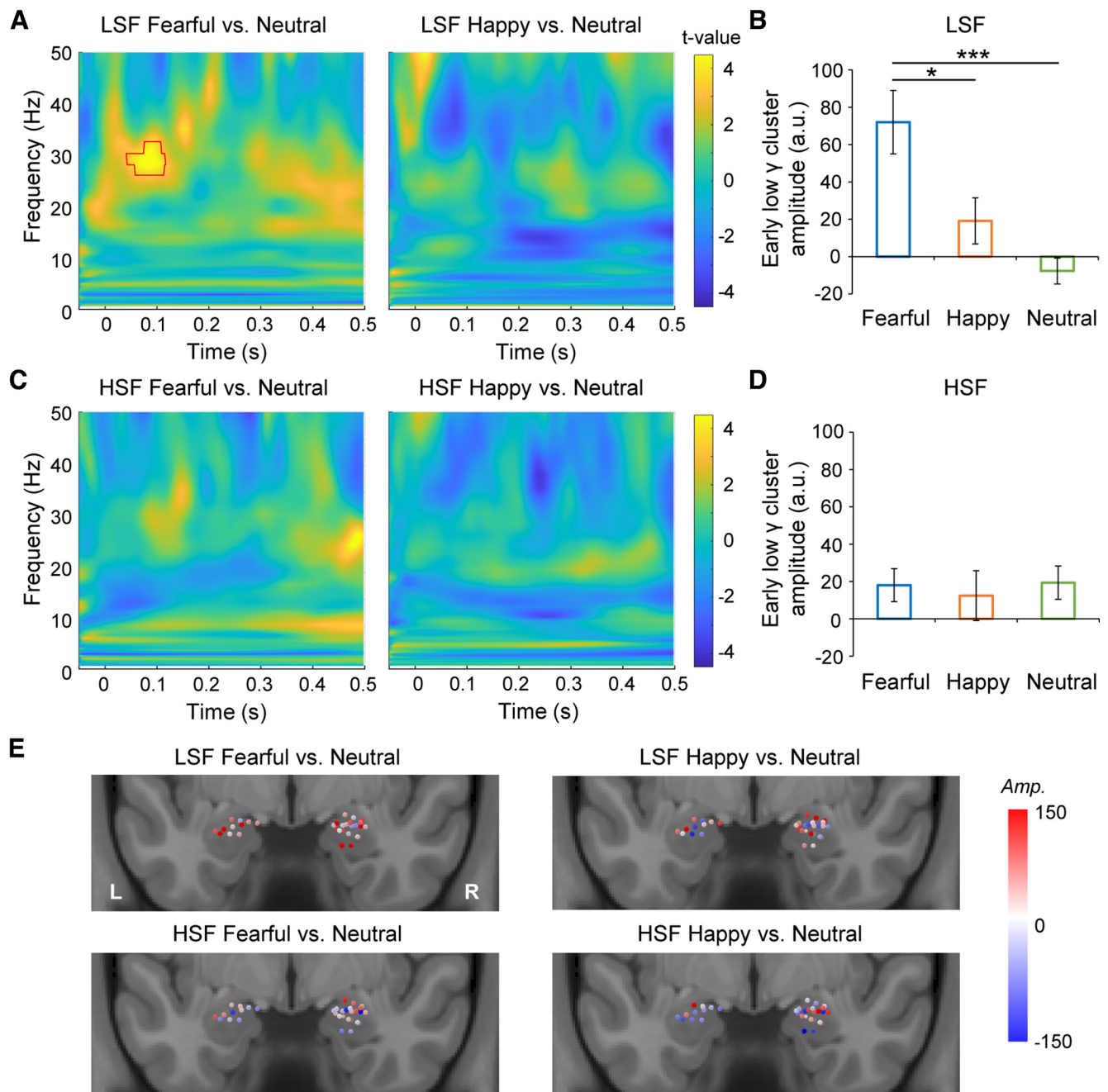


Figure 3. Time-frequency analyses of iEEGs in the amygdala. **A**, Statistical parametric maps of the time-frequency representation for the fearful (left) and happy (right) versus neutral face comparisons in the LSF condition. Red contour indicates the significant time-frequency cluster. **B**, Comparison of early low gamma amplitudes (a.u., arbitrary unit; frequency, 27–33 Hz; time, 45–118 ms) between the fearful/happy and neutral faces in the LSF condition. **C**, Statistical parametric maps of the time-frequency representation for the fearful (left) and happy (right) versus neutral face comparisons in the HSF condition. **D**, Comparison of early low gamma amplitudes between the fearful/happy and neutral faces in the HSF condition. **E**, The amplitude (Amp.) differences of the early low gamma cluster for single amygdala contacts. Error bars indicate SEM across contacts. *** $p < 0.001$, * $p < 0.05$ (two-tailed paired t tests, Bonferroni corrected).

0.01 (Fig. 2C, left). Meanwhile, no significant cluster was identified in the HSF condition (Fig. 2C, right). No response difference was observed between the happy and neutral face processing in either the LSF or HSF condition (Fig. 2C). We then compared the iERP responses between the LSF and HSF fearful faces. A significant cluster was identified showing a larger iERP response to the LSF than to the HSF fearful faces at an early latency (Fig. 2D, 50–202 ms).

To confirm the above findings, we extracted the iERP peak amplitude within the time window of 75–175 ms (Fig. 2C, gray shaded areas) for each emotion and SF condition. A linear

mixed-effects model that included the electrodes, amygdala sides, and patients as random factors was used to examine the iERP peak amplitude difference across the emotion conditions. We found a marginally significant emotion by SF interaction effect [$\chi^2(2) = 5.51, p = 0.064$]. Consistent with the finding in the cluster-based permutation test on iERP waveforms, the main effect of emotion was significant in the LSF condition [$\chi^2(2) = 9.16, p = 0.010$] but not in the HSF condition [$\chi^2(2) = 0.63, p = 0.731$]. Specifically, the peak amplitude was larger for the LSF fearful faces than for the LSF neutral faces (Fig. 2E, left; $t_{(32)} = 2.84, p = 0.024$ Bonferroni

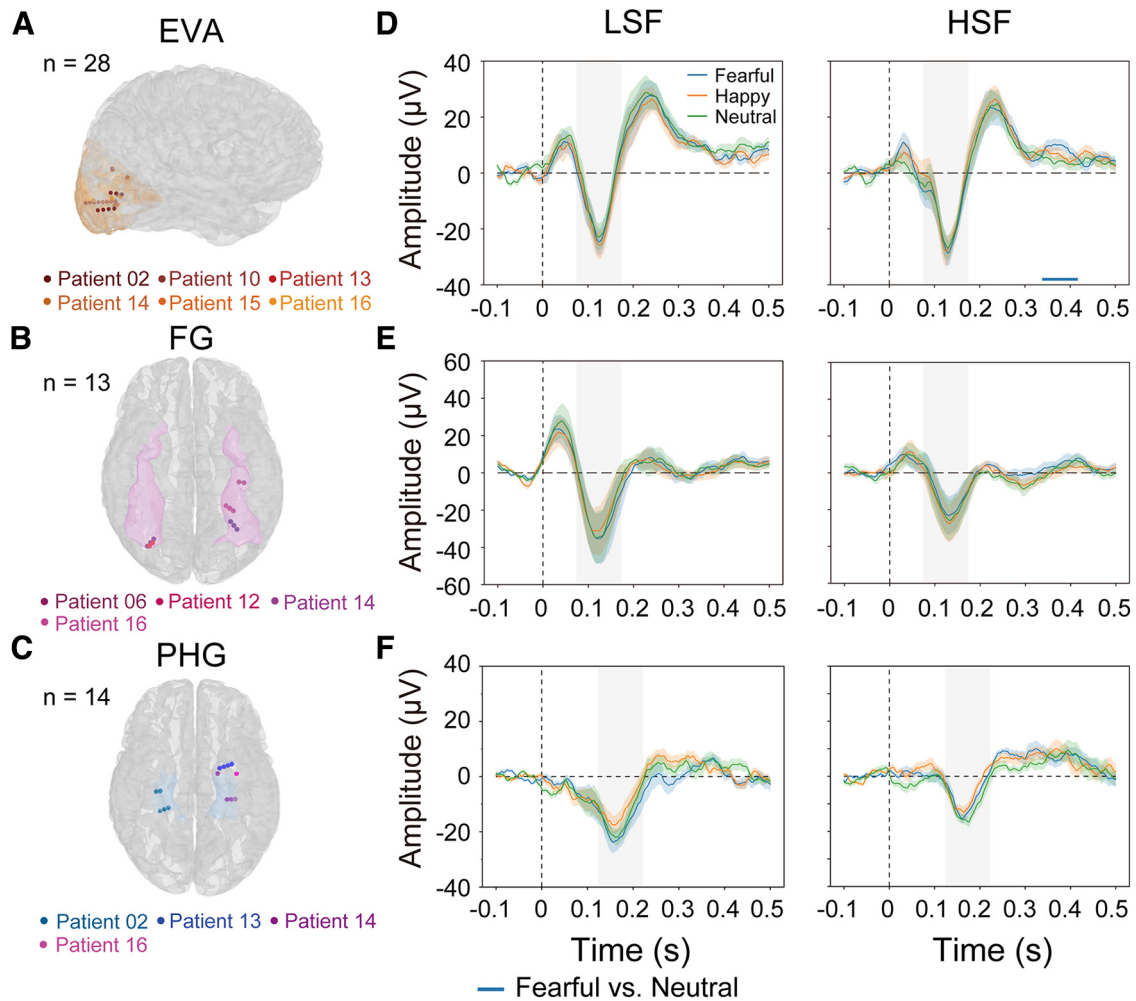


Figure 4. iERPs in visual cortex. *A–C*, Electrode contact locations in the EVAs (*A*), the FG (*B*), and the PHG (*C*). Contacts belonging to the same patient are depicted in the same color. *D–F*, iERPs to invisible fearful, happy, and neutral faces with only the LSF (left) or HSF (right) component in EVA, FG, and PHG. The horizontal bar indicates time clusters that show significant response differences between the fearful and neutral faces. The shaded areas around the iERP waveforms represent the SEM across contacts. The horizontal bar refers to the blue horizontal bar in Fig. 4*D* (right). The vertical shadings in *D–F* represent the 100-ms time window surrounding the iERP peak.

corrected, Cohen's $d = 0.49$). The peak amplitude difference between the LSF fearful and neutral faces was also significantly larger than that between the LSF happy and neutral faces (Fig. 2*E*, left; $t_{(32)} = 2.55$, $p = 0.048$ Bonferroni corrected, Cohen's $d = 0.44$). No peak amplitude difference between the fearful/happy faces and the neutral faces was observed with the HSF component (p values > 0.05 ; Fig. 2*E*, right). Altogether, these findings demonstrate a rapid, LSF-specific amygdala response to invisible fearful faces, supporting the subcortical emotion pathway model (Vuilleumier et al., 2003).

Rapid low gamma oscillations to invisible fearful faces

To further depict the frequency profiles of the iEEGs in the human amygdala, we performed a time-frequency analysis on the iEEGs in each emotion and SF condition. We found that the amygdala showed an early power increase (45–118 ms) at low gamma band (27–33 Hz) in response to the LSF fearful faces relative to the LSF neutral faces (Fig. 3*A*, left). Such a difference was not found in the LSF happy versus LSF neutral face comparison (Fig. 3*A*, right) or in the HSF condition (Fig. 3*C*). The mean amplitude of the early low gamma cluster was significantly higher for the LSF fearful faces than those for the LSF happy ($t_{(32)} = 2.68$, $p = 0.024$ Bonferroni corrected, Cohen's $d = 0.47$) and

neutral ($t_{(32)} = 4.50$, $p < 0.001$ Bonferroni corrected, Cohen's $d = 0.78$) faces (Fig. 3*B*). There was no difference in the HSF condition (Fig. 3*D*; p values > 0.05). We further visualized the amplitude differences of the early low gamma cluster for amygdala contacts on a brain template. As shown in Figure 3*E*, the effect was not localized to specific dominant contacts but was distributed across multiple contacts. Therefore, the rapid, LSF-specific amygdala response to the invisible fearful faces may be driven by the low gamma band oscillations.

No selective rapid response to invisible fearful faces in the visual cortex

Although the rapid LSF-specific amygdala response to the invisible fearful faces suggests a subcortical pathway for fear processing, it does not exclude the possibility that the fearful face information can be transmitted via cortical pathways. To examine this possibility, we analyzed cortical responses in patients who had electrode contacts in cortical regions along the ventral visual pathway, including the EVAs, the FG, and the PHG.

For the EVA contacts (Fig. 4*A*; 6 patients, 8 electrodes with 28 contacts in total), in contrast with the effects observed in the amygdala, we did not find any early effect in the LSF or HSF condition with the fearful/happy faces, relative to the neutral faces. A

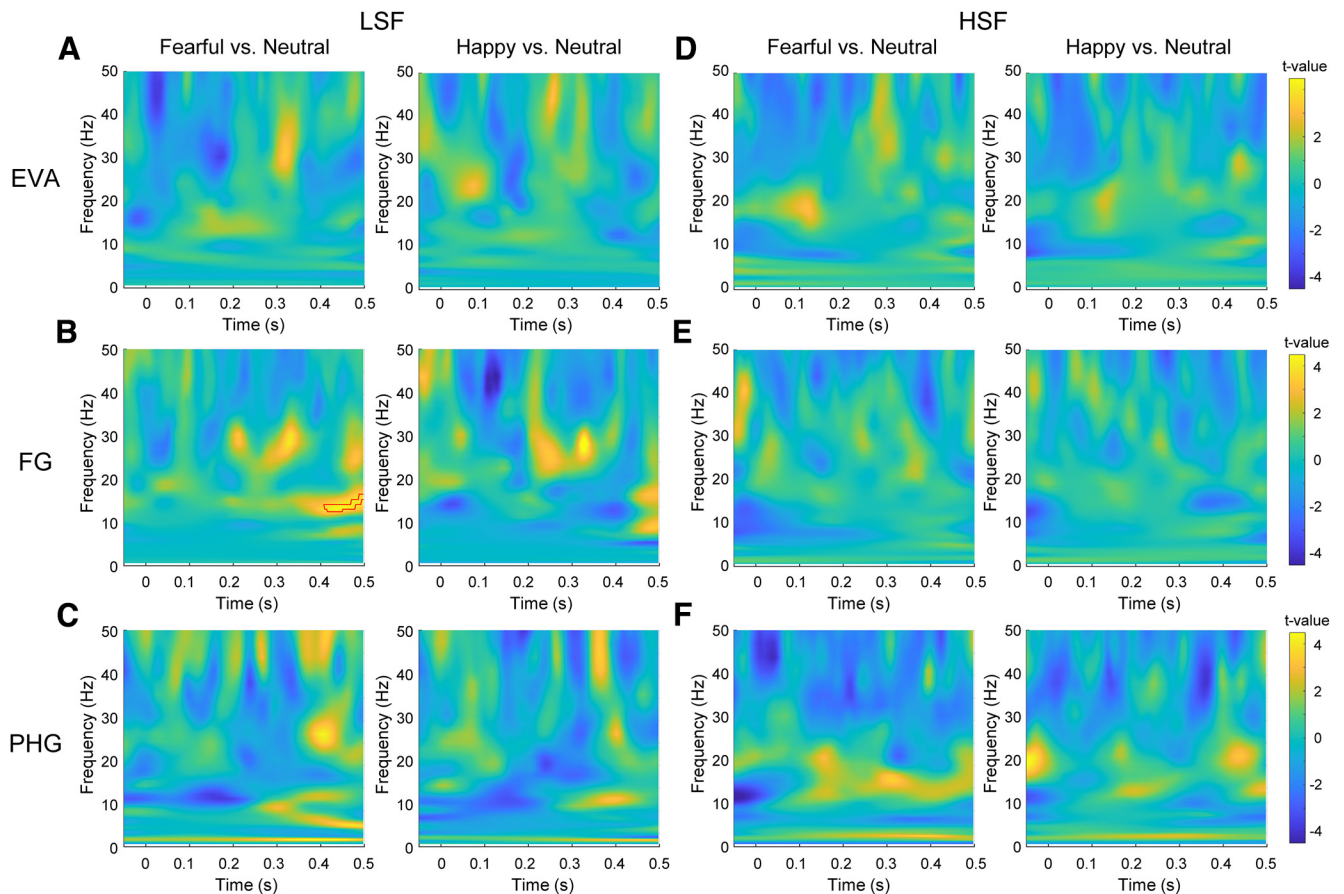


Figure 5. Time-frequency analyses of iEEGs in visual cortex. **A–F**, Statistical parametric maps of the time-frequency representation for the fearful/happy versus neutral face comparisons in the LSF condition in EVA (**A**), FG (**B**), and PHG (**C**) and those in the HSF condition in EVA (**D**), FG (**E**), and PHG (**F**). Red contour indicates the significant time-frequency cluster.

late-latency cluster (344–375 ms) was identified for the fearful versus neutral face comparison in the HSF condition, suggesting that the selectivity to HSF fearful faces emerged at a late stage (Fig. 4*D*, right). Next, we extracted the iERP peak amplitude within a 100 ms window surrounding the peak (i.e., 75–175 ms) for each emotion and SF condition (Fig. 4*D*, gray shaded areas). The linear mixed-effects model, same as that applied to the amygdala contacts, showed no emotion by SF interaction effect in the EVA [$\chi^2(2) = 0.05, p = 0.974$]. For the FG contacts (Fig. 4*B*; 4 patients, 5 electrodes with 13 contacts), no cluster showed significantly different iERPs to the fearful/happy versus neutral faces in either the LSF (Fig. 4*E*, left) or the HSF (Fig. 4*E*, right) condition. No emotion by SF interaction was found with the peak amplitudes [Fig. 4*E*, gray shaded areas; 75–175 ms, $\chi^2(2) = 3.69, p = 0.158$] either. For the PHG contacts (Fig. 4*C*; 4 patients, 6 electrodes with 14 contacts), no early effect was found for the fearful/happy faces relative to the neutral faces, and no emotion by SF interaction was found with the peak amplitudes [Fig. 4*F*, gray shaded areas; 125–225 ms, $\chi^2(2) = 1.17, p = 0.556$] either. Because the effects in the early visual cortex occurred much later than those in the amygdala, they could not explain the rapid response in the amygdala.

We further performed time-frequency analyses on cortical iEEGs. As shown in Figure 5, no early effects were found for the fearful/happy versus neutral face comparisons in EVA (Fig. 5*A, D*), FG (Fig. 5*B, E*), or PHG (Fig. 5*C, F*) in either the LSF or the HSF condition. Only late effects at the beta band were found in FG (Fig. 5*B*). Collectively, the absence of rapid responses to

invisible LSF fearful faces in the ventral cortical stream argues against the possibility that the rapid discrimination of invisible fearful faces in the amygdala arises from neural activities in EVA, FG, or PHG.

Discussion

Subcortical sensory pathways have been suggested to be sufficient for rapid and unconscious processing of ecologically important stimuli, but direct electrophysiological support is lacking. Here, we reported intracranial ERP evidence that the human amygdala could selectively process invisible fearful faces containing only low spatial frequency information at an early latency of ~ 88 ms. Time-frequency analyses further identified that the rapid fear detection in the amygdala was associated with increased power at the low gamma frequency band. Critically, such early fear-selective responses were absent in cortical areas along the ventral visual pathway, excluding their contribution to the amygdala response. These findings strongly support the low-road model suggesting that threat information can be transmitted through a subcortical magnocellular route to the amygdala independent of the cortical pathways in humans.

Controversies remain over the response latency of the amygdala to fear. Although rapid amygdala responses to visible fearful or threatening stimuli have been reported within 100 ms after stimulus onset in magnetoencephalogram (MEG) studies (Luo et al., 2007, 2009, 2010; Bayle et al., 2009; Maratos et al., 2009; Hung et al., 2010; McFadyen et al., 2017), single-neuron and iEEG recordings in the monkey (Gothard et al.,

2007) and human (Oya et al., 2002; Krolak-Salmon et al., 2004; Mormann et al., 2008; Pourtois et al., 2010) amygdala mostly reported responses at a latency later than 100 ms. Potentially benefiting from the use of a larger sample size and more recording trials, an earlier human iEEG study found a faster amygdala response to fearful than to happy and neutral faces at 74 ms after stimulus onset (Méndez-Bértolo et al., 2016). The 88 ms effect latency to LSF fearful faces in our study is consistent with this result and extends this effect to invisible stimuli. We further identified that the rapid amygdala response emerged at the low gamma frequency band at an earlier latency of 45 ms. Previous studies have also associated the gamma band power increase occurring at a latency as early as ~50 ms in the subcortical structures, including the superior colliculus, pulvinar, and the amygdala, with face and emotion processing (Oya et al., 2002; Sato et al., 2011; Le et al., 2019). Here, the low gamma band effect was earlier than that found in iERPs. Considering that the iERPs are broadband signals, the rapid low gamma effect might be swamped by noise in other frequency bands, resulting in the delayed effect onset in the iERPs (Sato et al., 2011). This can also explain previous inconsistent findings in iERP studies (Allison et al., 1999; Krolak-Salmon et al., 2004). Together, the human amygdala is likely to discriminate fearful from neutral faces within 100 ms, regardless of the stimulus visibility.

The evidence for rapid amygdala response alone is not sufficient to support the subcortical pathway model. The multiroad model has suggested that subcortical visual processing is not necessarily faster than cortical processing (Pessoa and Adolphs, 2010). This model suggests that there exist shortcut connections in the corticocortical and subcortico-cortical pathways so that transmission of emotional information could be implemented rapidly. Although this assumption is tempting, direct evidence for the multiroad model is lacking. The multiroad hypothesis is difficult to be falsified by the iEEG technique. Because of the limited number of recording sites, it is hard to exhaust all potential shortcuts for the cortical pathway to the amygdala. Probing unconscious processing is an ideal way to examine the low-road and the multiroad models. First, subcortical regions have been found to be preferentially recruited for unconscious rather than conscious visual processing. In fear conditioning, invisible conditioned faces activated the amygdala more than visible faces. Likewise, an invisible conditioned stimulus could induce coactivation among the amygdala, the superior colliculus, and the pulvinar, but the coactivation was not apparent if the conditioned stimulus was visible (Morris et al., 1998a, 1999). In contrast, invisible faces are either insufficient to evoke cortical responses or evoke very weak cortical responses, especially in the ventral visual pathway (Jiang and He, 2006; Tamietto and de Gelder, 2010; Axelrod et al., 2015), suggesting that the cortical visual pathway is not a major source of the amygdala response to invisible stimuli. These findings are consistent with our finding of LSF specificity, a feature of subcortical information transmission, in the amygdala but not in cortical areas along the ventral visual pathway to invisible fear. It should be noted that because the dorsal visual pathway can process invisible visual information (Fang and He, 2005; Jiang and He, 2006; Mo et al., 2022), future studies should investigate the potential contribution of cortical regions in the dorsal pathway to the rapid amygdala response, even though the dorsal pathway is not sensitive to face information (Fang and He, 2005).

The present finding on invisible fear complements the literature on rapid emotion processing in the amygdala. The rapid

amygdala response to invisible fearful faces and the absence of early effects in the visual cortices demonstrate the existence of a subcortical pathway independent of cortical inputs. Such a subcortical pathway for unconscious fear detection has ecological advantages, allowing detection of coarse emotional information even when the cortical pathway is unavailable. So far, rapid, selective amygdala response has been demonstrated in both visible and invisible fear processing, with direct and indirect measures (Sato et al., 2011; Garrido et al., 2012; Méndez-Bértolo et al., 2016; McFadyen et al., 2017). Although both visible and invisible fear information recruits the subcortical pathway, they could still be segregated and transmitted to different subparts of the amygdala (Liddell et al., 2004; Williams et al., 2004, 2006). For instance, it has been shown that the dorsal amygdala exhibited dominant activation to visible fearful faces. In contrast, the ventral amygdala was more active to faces rendered invisible by binocular suppression (Lerner et al., 2012). There is also evidence that implicit and explicit fear processing activate different sides of the amygdala (Morris et al., 1998b; Williams et al., 2006). More studies are needed to explore the interaction between cortical and subcortical pathways during visible and invisible threat information processing.

We found that the rapid amygdala response is specific to the LSF face component. This is in line with the low-road model that the amygdala receives coarse visual information through a subcortical magnocellular route sensitive to LSF information (Pessoa and Adolphs, 2010). In contrast to the LSF specificity in the amygdala response, the EVA showed specificity to HSF fear in the iERP result. This dissociation between subcortical and cortical structures in SF has previously been reported in fMRI studies that showed larger signals to LSF than HSF fearful faces in the superior colliculus, pulvinar, and amygdala, and larger signals to HSF faces in the extrastriate visual cortex (Vuilleumier et al., 2003). The fMRI evidence, however, could not provide sufficient temporal information. Although MEG could overcome this problem, it cannot directly measure the activities of deep brain structures. So researchers have used indirect methods such as dynamic causal modeling on MEG data to examine information transmission to the amygdala (Garrido et al., 2012). Recent studies demonstrated a pulvinar-amygdala connection supporting rapid emotion processing, but the connection was not affected by SF (McFadyen et al., 2017, 2019). Because of the low spatial resolution of MEG, this could be because of that, the human pulvinar receives both magnocellular and parvocellular retinal inputs (Cowey et al., 1994) and transmits information to the amygdala through multiple pathways (Pessoa and Adolphs, 2010; Diano et al., 2017). The iEEG recording overcomes these problems of the traditional neuroimaging techniques. With direct evidence from iEEG recording, Méndez-Bértolo et al., (2016) and we all argue that the amygdala preferentially processes LSF information.

Our results provide conclusive evidence for the rapid processing of invisible fearful faces in the human amygdala. This rapid processing is specific to the low spatial frequency component and is independent of cortical regions in the ventral pathway, supporting the existence of a functionally independent subcortical pathway for automatic fear processing.

References

- Allison T, Puce A, Spencer DD, McCarthy G (1999) Electrophysiological studies of human face perception. I: potentials generated in occipitotemporal cortex by face and non-face stimuli. *Cereb Cortex* 9:415–430.

- Axelrod V, Bar M, Rees G (2015) Exploring the unconscious using faces. *Trends Cogn Sci* 19:35–45.
- Bayle DJ, Henaff M-A, Krolak-Salmon P (2009) Unconsciously perceived fear in peripheral vision alerts the limbic system: a MEG study. *PLoS One* 4:e8207.
- Benson NC, Butt OH, Brainard DH, Aguirre GK (2014) Correction of distortion in flattened representations of the cortical surface allows prediction of V1–V3 functional organization from anatomy. *PLoS Comput Biol* 10:e1003538.
- Brainard D (1997) The Psychophysics Toolbox. *Spat Vis* 10:433–436.
- Brooks SJ, Savov V, Allzén E, Benedict C, Fredriksson R, Schiöth HB (2012) Exposure to subliminal arousing stimuli induces robust activation in the amygdala, hippocampus, anterior cingulate, insular cortex and primary visual cortex: a systematic meta-analysis of fMRI studies. *Neuroimage* 59:2962–2973.
- Cowey A, Stoerig P, Bannister M (1994) Retinal ganglion cells labelled from the pulvinar nucleus in macaque monkeys. *Neuroscience* 61:691–705.
- Dale AM, Fischl B, Sereno MI (1999) Cortical surface-based analysis. *Neuroimage* 9:179–194.
- Degonda N, Mondadori CRA, Bosshardt S, Schmidt CF, Boesiger P, Nitsch RM, Hock C, Henke K (2005) Implicit associative learning engages the hippocampus and interacts with explicit associative learning. *Neuron* 46:505–520.
- Diano M, Celeghin A, Bagnis A, Tamietto M (2017) Amygdala response to emotional stimuli without awareness: facts and interpretations. *Front Psychol* 7:2029.
- Fang F, He S (2005) Cortical responses to invisible objects in the human dorsal and ventral pathways. *Nat Neurosci* 8:1380–1385.
- Garrido MI, Barnes GR, Sahani M, Dolan RJ (2012) Functional evidence for a dual route to amygdala. *Curr Biol* 22:129–134.
- Gothard KM, Battaglia FP, Erickson CA, Spitzer KM, Amaral DG (2007) Neural responses to facial expression and face identity in the monkey amygdala. *J Neurophysiol* 97:1671–1683.
- Hung Y, Smith ML, Bayle DJ, Mills T, Cheyne D, Taylor MJ (2010) Unattended emotional faces elicit early lateralized amygdala–frontal and fusiform activations. *Neuroimage* 50:727–733.
- Jiang Y, He S (2006) Cortical responses to invisible faces: dissociating subsystems for facial-information processing. *Curr Biol* 16:2023–2029.
- Joshi AA, Choi S, Liu Y, Chong M, Sonkar G, Gonzalez-Martinez J, Nair D, Wisnowski JL, Haldar JP, Shattuck DW, Damasio H, Leahy RM (2022) A hybrid high-resolution anatomical MRI atlas with sub-parcellation of cortical gyri using resting fMRI. *J Neurosci Methods* 374:109566.
- Krolak-Salmon P, Henaff M-A, Vighetto A, Bertrand O, Mauguère F (2004) Early amygdala reaction to fear spreading in occipital, temporal, and frontal cortex: a depth electrode ERP study in human. *Neuron* 42:665–676.
- Le QV, Nishimaru H, Matsumoto J, Takamura Y, Nguyen MN, Mao CV, Hori E, Maior RS, Tomaz C, Ono T, Nishijo H (2019) Gamma oscillations in the superior colliculus and pulvinar in response to faces support discrimination performance in monkeys. *Neuropsychologia* 128:87–95.
- LeDoux JE (1996) *The emotional brain: The mysterious underpinnings of emotional life*. New York: Simon & Schuster.
- Lerner Y, Singer N, Gonen T, Weintraub Y, Cohen O, Rubin N, Ungerleider LG, Hendler T (2012) Feeling without seeing? engagement of ventral, but not dorsal, amygdala during unaware exposure to emotional faces. *J Cogn Neurosci* 24:531–542.
- Liddell BJ, Williams LM, Rathjen J, Shevlin H, Gordon E (2004) A temporal dissociation of subliminal versus supraliminal fear perception: an event-related potential study. *J Cogn Neurosci* 16:479–486.
- Lu J, Luo L, Wang Q, Fang F, Chen N (2021) Cue-triggered activity replay in human early visual cortex. *Sci China Life Sci* 64:144–151.
- Luo Q, Holroyd T, Jones M, Hendler T, Blair J (2007) Neural dynamics for facial threat processing as revealed by gamma band synchronization using MEG. *Neuroimage* 34:839–847.
- Luo Q, Mitchell D, Cheng X, Mondillo K, Mccaffrey D, Holroyd T, Carver F, Coppola R, Blair J (2009) Visual awareness, emotion, and gamma band synchronization. *Cereb Cortex* 19:1896–1904.
- Luo Q, Holroyd T, Majestic C, Cheng X, Schechter J, Blair RJ (2010) Emotional automaticity is a matter of timing. *J Neurosci* 30:5825–5829.
- Maratos FA, Mogg K, Bradley BP, Rippon G, Senior C (2009) Coarse threat images reveal theta oscillations in the amygdala: a magnetoencephalography study. *Cogn Affect Behav Neurosci* 9:133–143.
- Maris E, Oostenveld R (2007) Nonparametric statistical testing of EEG- and MEG-data. *J Neurosci Methods* 64:177–190.
- McFadyen J, Mermillod M, Mattingley JB, Halász V, Garrido MI (2017) A rapid subcortical amygdala route for faces irrespective of spatial frequency and emotion. *J Neurosci* 37:3864–3874.
- McFadyen J, Mattingley JB, Garrido MI (2019) An afferent white matter pathway from the pulvinar to the amygdala facilitates fear recognition. *Elife* 8:e40766.
- Méndez-Bértolo C, Moratti S, Toledano R, Lopez-Sosa F, Martínez-Alvarez R, Mah YH, Vuilleumier P, Gil-Nagel A, Strange BA (2016) A fast pathway for fear in human amygdala. *Nat Neurosci* 19:1041–1049.
- Mo C, Lu J, Shi C, Fang F (2022) Neural representations of competing stimuli along the dorsal and ventral visual pathways during binocular rivalry. *Cereb Cortex*. Advance online publication. Retrieved January 7, 2023. <https://doi.org/10.1093/cercor/bhac238>.
- Mormann F, Kornblith S, Quiroga RQ, Kraskov A, Cerf M, Fried I, Koch C (2008) Latency and selectivity of single neurons indicate hierarchical processing in the human medial temporal lobe. *J Neurosci* 28:8865–8872.
- Morris JS, Friston KJ, Büchel C, Frith CD, Young AW, Calder AJ, Dolan RJ (1998a) A neuromodulatory role for the human amygdala in processing emotional facial expressions. *Brain* 121:47–57.
- Morris JS, Öhman A, Dolan RJ (1998b) Conscious and unconscious emotional learning in the human amygdala. *Nature* 393:467–470.
- Morris JS, Öhman A, Dolan RJ (1999) A subcortical pathway to the right amygdala mediating “unseen” fear. *Proc Natl Acad Sci U S A* 96:1680–1685.
- Morris JS, DeGelder B, Weiskrantz L, Dolan RJ (2001) Differential extrageniculostriate and amygdala responses to presentation of emotional faces in a cortically blind field. *Brain* 124:1241–1252.
- Oostenveld R, Fries P, Maris E, Schoffelen J-M (2011) FieldTrip: open source software for advanced analysis of MEG, EEG, and invasive electrophysiological data. *Comput Intell Neurosci* 2011:156869–156869.
- Oya H, Kawasaki H, Howard MA, Adolphs R (2002) Electrophysiological responses in the human amygdala discriminate emotion categories of complex visual stimuli. *J Neurosci* 22:9502–9512.
- Pessoa L, Adolphs R (2010) Emotion processing and the amygdala: from a “low road” to “many roads” of evaluating biological significance. *Nat Rev Neurosci* 11:773–783.
- Pessoa L, Japee S, Ungerleider LG (2005) Visual awareness and the detection of fearful faces. *Emotion* 5:243–247.
- Phan KL, Wager T, Taylor SF, Liberzon I (2002) Functional neuroanatomy of emotion: a meta-analysis of emotion activation studies in PET and fMRI. *Neuroimage* 16:331–348.
- Pourtois G, Spinelli L, Seck M, Vuilleumier P (2010) Temporal precedence of emotion over attention modulations in the lateral amygdala: intracranial ERP evidence from a patient with temporal lobe epilepsy. *Cogn Affect Behav Neurosci* 10:83–93.
- Sato W, Kochiyama T, Uono S, Matsuda K, Usui K, Inoue Y, Toichi M (2011) Rapid amygdala gamma oscillations in response to fearful facial expressions. *Neuropsychologia* 49:612–617.
- Tadel F, Baillet S, Mosher JC, Pantazis D, Leahy RM (2011) Brainstorm: a user-friendly application for MEG/EEG analysis. *Comput Intell Neurosci* 2011:879716.
- Tamietto M, de Gelder B (2010) Neural bases of the non-conscious perception of emotional signals. *Nat Rev Neurosci* 11:697–709.
- Tamietto M, Castelli L, Vighetti S, Perozzo P, Geminiani G, Weiskrantz L, de Gelder B (2009) Unseen facial and bodily expressions trigger fast emotional reactions. *Proc Natl Acad Sci U S A* 106:17661–17666.
- Tamietto M, Pullens P, de Gelder B, Weiskrantz L, Goebel R (2012) Subcortical connections to human amygdala and changes following destruction of the visual cortex. *Curr Biol* 22:1449–1455.
- Vuilleumier P, Armony JL, Driver J, Dolan RJ (2003) Distinct spatial frequency sensitivities for processing faces and emotional expressions. *Nat Neurosci* 6:624–631.
- Whalen PJ, Rauch SL, Etcoff NL, McInerney SC, Lee MB, Jenike MA (1998) Masked presentations of emotional facial expressions modulate amygdala activity without explicit knowledge. *J Neurosci* 18:411–418.
- Williams MA, Morris AP, McGlone F, Abbott DF, Mattingley JB (2004) Amygdala responses to fearful and happy facial expressions under conditions of binocular suppression. *J Neurosci* 24:2898–2904.
- Williams LM, Liddell BJ, Kemp AH, Bryant RA, Meares RA, Peduto AS, Gordon E (2006) Amygdala–prefrontal dissociation of subliminal and supraliminal fear. *Hum Brain Mapp* 27:652–661.